Advances in Difference Equations
a SpringerOpen Journal

RESEARCH **Open Access**

Numerical solution of nonlinear stochastic Itô–Volterra integral equations based on Haar wavelets

Jieheng Wu[1], Guo Jiang[1*] and Xiaoyan Sang[1]

*Correspondence:
gjiang@hbnu.edu.cn
[1]School of Mathematics and
Statistics, Hubei Normal University,
Huangshi, P.R. China

Abstract

In this paper, an efficient numerical method is presented for solving nonlinear stochastic Itô–Volterra integral equations based on Haar wavelets. By the properties of Haar wavelets and stochastic integration operational matrixes, the approximate solution of nonlinear stochastic Itô–Volterra integral equations can be found. At the same time, the error analysis is established. Finally, two numerical examples are offered to testify the validity and precision of the presented method.

Keywords: Haar wavelets; Stochastic integration operational matrixes; Stochastic Itô–Volterra integral equations

1 Introduction

Stochastic integral equations are widely applied in engineering, biology, oceanography, physical sciences, etc. There systems are dependent on a noise source, such as Gaussian white noise. As we all know, many stochastic Volterra integral equations do not have exact solutions, so it makes sense to find more precise approximate solutions to stochastic Volterra integral equations. There are different numerical methods to stochastic Volterra integral equations, for example, orthogonal basis methods [1–10], wash series methods [11, 12], and polynomials methods [13–16].

In [1], Fakhrodin studied linear stochastic Itô–Volterra integral equations (SIVIEs) through Haar wavelets (HWs). In [3], Maleknejad et al. also considered the same integral equations by applying block pulse functions (BPFs). In [9], Heydari et al. solved linear SIVIEs by the generalized hat basis functions. Meanwhile, in line with the same hat functions, Hashemi et al. also presented the numerical method of nonlinear SIVIEs driven by fractional Brownian motion [8]. Moreover, Jiang et al. applied BPFs to solve two-dimensional nonlinear SIVIEs [7]. In a general way, Zhang studied the existence and uniqueness solution to stochastic Volterra integral equations with singular kernels and constructed an Euler type approximation solution [17, 18].

Inspired by the discussion above, we use HWs to solve the following nonlinear SIVIE:

$$x(v) = x_0(v) + \int_0^v k(u,v)\sigma\big(x(u)\big)\,du + \int_0^v r(u,v)\rho\big(x(u)\big)\,dB(u), \quad v \in [0,1), \tag{1}$$

where $x(v)$ is an unknown stochastic process defined on some probability space $(\Omega, \mathcal{F}, P)$, $k(u, v)$ and $r(u, v)$ are kernel functions for $u, v \in [0, 1)$, and $x_0(v)$ is an initial value function. $B(u)$ is a Brownian motion and $\int_0^v r(u, v)\rho(x(u)) \, dB(u)$ is Itô integral. σ and ρ are analytic functions that satisfy some bounded and Lipschitz conditions.

In contrast to the above papers [1, 3, 7–9], the differences of this paper are as follows. Firstly, we construct a preparation theorem to deal with the nonlinear analytic functions. Secondly, the error analysis is strictly proved. Finally, compared with the reference [8], the numerical solution is more accurate and the calculation is simpler because of the use of HWs. Moreover, the rationality and effectiveness of this method can be further supported by two examples.

The structure of the article is as follows.

In Sect. 2, some preliminaries of BPFs and HWs are given. In Sect. 3, the relationship between HWs and BPFs is shown. In Sect. 4, the approximate solutions of (1) are derived. In Sect. 5, the error analysis of the numerical method is demonstrated. In Sect. 6, the validity and efficiency of the numerical method are verified by two examples.

2 Preliminaries

BPFs and HWs have been widely analysed by lots of scholars. For details, see references [1, 3].

2.1 Block pulse functions

BPFs are denoted as

$$
\psi_i(v) = \begin{cases} 1 & ih \leq v < (i+1)h, \\ 0 & \text{otherwise}, \end{cases}
$$

for $i = 0, \ldots, m-1$, $m = 2^L$ for a positive integer L and $h = \frac{1}{m}$, $v \in [0, 1)$.

The basic properties of BPFs are shown as follows:

(i) disjointness:

$$
\psi_i(v)\psi_j(v) = \delta_{ij}\psi_i(v), \tag{2}
$$

where $v \in [0, 1)$, $i, j = 0, 1, \ldots, m-1$, and δ_{ij} is Kronecker delta;

(ii) orthogonality:

$$
\int_0^T \psi_i(v)\psi_j(v) \, dt = h\delta_{ij};
$$

(iii) completeness property: for every $g \in L^2[0, 1)$, Parseval's identity satisfies

$$
\int_0^1 g^2(v) \, dv = \lim_{m \to \infty} \sum_{i=0}^m (g_i)^2 \|\psi_i(v)\|^2, \tag{3}
$$

where

$$
g_i = \frac{1}{h} \int_0^1 g(v)\psi_i(v) \, dv.
$$

The set of BPFs can be represented by the following m-dimensional vector:

$$\Psi_m(v) = \big(\psi_0(v), \ldots, \psi_{m-1}(v)\big)^T, \quad v \in [0, 1). \tag{4}$$

From the above description, it yields

$$\Psi_m(v)\Psi_m^T(v) = \begin{pmatrix} \psi_0(v) & 0 & \cdots & 0 \\ 0 & \psi_1(v) & \cdots & 0 \\ \vdots & \vdots & \ddots & \vdots \\ 0 & 0 & \cdots & \psi_{m-1}(v) \end{pmatrix}_{m \times m},$$

$$\Psi_m^T(v)\Psi_m(v) = 1,$$

$$\Psi_m(v)\Psi_m^T(v)F_m = \mathbf{D}_{F_m}\Psi_m(v),$$

where $F_m = (f_0, f_1, \ldots, f_{m-1})^T$ and $\mathbf{D}_{F_m} = \mathrm{diag}(F_m)$.

Furthermore, for an $m \times m$ matrix $\mathbf{M}$, it yields

$$\Psi_m^T(v)\mathbf{M}\Psi_m(v) = \hat{M}^T\Psi_m(v),$$

where $\hat{M}$ is an m-dimensional vector and its entries equal the main diagonal entries of $\mathbf{M}$.

In accordance with BPFs, every function $x(v)$ which satisfies square integrable conditions in the interval $[0, 1)$ can be approached as follows:

$$x(v) \simeq x_m(v) = \sum_{i=0}^{m-1} x_i\psi_i(v) = X_m^T\Psi_m(v) = \Psi_m^T(v)X_m,$$

where the function $x_m(v)$ is an approximation of the function $x(v)$ and

$$X_m = (x_0, x_1, \ldots, x_{m-1})^T. \tag{5}$$

Similarly, every function $k(u, v)$ defined on $[0, 1) \times [0, 1)$ can be written as

$$k(u, v) = \Psi_{m_1}^T(u)\mathbf{K}\Phi_{m_2}(v),$$

where $\mathbf{K} = (k_{ij})_{m_1 \times m_2}$ with

$$k_{ij} \simeq \frac{1}{h_1 h_2} \int_0^1 \int_0^1 k(u, v)\psi_i(u)\phi_j(v)\, du\, dv, \tag{6}$$

and $h_1 = \frac{1}{m_1}$, $h_2 = \frac{1}{m_2}$.

2.2 Haar wavelets

The notation and definition of HWs are introduced in this section (also see [1]). The set of orthogonal HWs is defined as follows:

$$h_i(v) = 2^{\frac{l}{2}}h\big(2^l v - z\big), \quad i = 2^l + z, 0 \le z < 2^l, l \ge 0, i, l, z \in \mathbb{N},$$

where $h_0(v) = 1$, $v \in [0, 1)$, and

$$h(v) = \begin{cases} 1 & 0 \le v < \frac{1}{2}, \\ -1 & \frac{1}{2} \le v < 1. \end{cases}$$

For HWs $h_n(v)$ defined in $[0, 1)$, we have

$$\int_0^1 h_i(v)h_j(v)\,dv = \delta_{ij}, \tag{7}$$

where δ_{ij} is the Kronecker delta.

In accordance with HWs, every function $x(v)$ that satisfies square integrable conditions can be approached as follows:

$$x(v) = c_0 h_0(v) + \sum_{i=1}^{\infty} c_i h_i(v), \quad v \in [0, 1), i = 2^l + z, 0 \le z < 2^l, l \ge 0, l, z \in \mathbb{N}, \tag{8}$$

where

$$c_i = \int_0^1 x(v)h_i(v)\,dv, \quad i = 0 \quad \text{or} \quad i = 2^l + z, 0 \le z < 2^l, l \ge 0, l, z \in \mathbb{N}. \tag{9}$$

We can see that when $m = 2^L$, equation (8) can be rewritten as

$$x(v) = c_0 h_0(v) + \sum_{i=1}^{m-1} c_i h_i(v), \quad i = 2^l + z, 0 \le z < 2^l, l = 0, 1, \dots, L - 1.$$

Obviously, the vector form is as follows:

$$x(v) \simeq C_m^T H_m(v) = H_m^T(v)C_m, \tag{10}$$

where $H_m = (h_0(v), h_1(v), \dots, h_{m-1}(v))^T$ and $C_m = (c_0, c_1, \dots, c_{m-1})^T$ are HWs and Haar coefficients, respectively.

Similarly, every function $k(u, v)$ defined on $[0, 1) \times [0, 1)$ can be approached as follows:

$$k(u, v) = H_m^T(u)\mathbf{K}H_m(v),$$

where $\mathbf{K} = (k_{ij})_{m \times m}$ with

$$k_{ij} = \int_0^1 \int_0^1 k(u, v)h_i(u)h_j(v)\,du\,dv, \quad i, j = 0, 1, \dots, m - 1.$$

3 Haar wavelets and BPFs

Some lemmas about HWs and BPFs are introduced in this section. For a detailed description, see the reference [1].

Lemma 3.1 *Suppose that $H_m(v)$ and $\Psi_m(v)$ are respectively given in (10) and (4), $H_m(v)$ can be written in accordance with BPFs as follows:*

$$H_m(v) = \mathbf{Q}\Psi_m(v), \quad m = 2^L, \tag{11}$$

where $\mathbf{Q} = (Q_{ij})_{m \times m}$ and

$$Q_{ij} = 2^{\frac{i}{2}} h_{i-1}\left(\frac{2j-1}{2m}\right), \quad i,j = 1, 2, \ldots, m, i - 1 = 2^l + z, 0 \le z < 2^l.$$

Proof See [1]. □

Lemma 3.2 *Suppose that* $\mathbf{Q}$ *is given in* (11), *then we have*

$$\mathbf{Q}^T \mathbf{Q} = m\mathbf{I},$$

where $\mathbf{I}$ *is an* $m \times m$ *identity matrix.*

Proof See [1]. □

Lemma 3.3 *Suppose that* F *is an* m-*dimensional vector, we have*

$$H_m(v)H_m^T(v)F = \tilde{\mathbf{F}}H_m(v),$$

where $\tilde{\mathbf{F}}$ *is an* $m \times m$ *matrix and* $\tilde{\mathbf{F}} = \mathbf{Q}\bar{\mathbf{F}}\mathbf{Q}^{-1}$, $\bar{\mathbf{F}} = \text{diag}(\mathbf{Q}^T F)$.

Proof See [1]. □

Lemma 3.4 *Suppose that* $\mathbf{M}$ *is an* $m \times m$ *matrix, we have*

$$H_m^T(v)\mathbf{M}H_m(v) = \hat{M}H_m(v),$$

where $\hat{M} = N^T \mathbf{Q}^{-1}$ *is an* m-*dimensional vector and the entries of the vector* N *are the diagonal entries of matrix* $\mathbf{Q}^T \mathbf{M} \mathbf{Q}$.

Proof See [1]. □

Lemma 3.5 *Suppose that* $\Psi_m(v)$ *is given in* (4), *we have*

$$\int_0^v \Psi_m(u)\,du \simeq \mathbf{P}\Psi_m(v),$$

where

$$\mathbf{P} = \frac{h}{2}\begin{pmatrix} 1 & 2 & 2 & \cdots & 2 \\ 0 & 1 & 2 & \cdots & 2 \\ 0 & 0 & 1 & \cdots & 2 \\ \vdots & \vdots & \vdots & \ddots & \vdots \\ 0 & 0 & 0 & \cdots & 1 \end{pmatrix}_{m \times m}.$$

Proof See [1, 3]. □

Lemma 3.6 *Suppose that $\Psi_m(v)$ is given in* (4), *we have*

$$\int_0^v \Psi_m(u)\,dB(u) \simeq \mathbf{P}_B \Psi_m(v),$$

where

$$\mathbf{P}_B = \begin{pmatrix} B(\frac{h}{2}) & B(h) & B(h) & \cdots & B(h) \\ 0 & B(\frac{3h}{2})-B(h) & B(2h)-B(h) & \cdots & B(2h)-B(h) \\ 0 & 0 & B(\frac{5h}{2})-B(2h) & \cdots & B(3h)-B(2h) \\ \vdots & \vdots & \vdots & \ddots & \vdots \\ 0 & 0 & 0 & \cdots & B(\frac{(2m-1)h}{2})-B((m-1)h) \end{pmatrix}_{m\times m}.$$

Proof See [1, 3]. $\qquad\square$

Lemma 3.7 *Suppose that $H_m(v)$ is given in* (10), *we have*

$$\int_0^v H_m(u)\,du \simeq \frac{1}{m}\mathbf{Q}\mathbf{P}\mathbf{Q}^T H_m(v) = \Lambda H_m(v),$$

where $\mathbf{Q}$ and $\mathbf{P}$ are respectively given in (11) *and Lemma* 3.3, $\Lambda = \frac{1}{m}\mathbf{Q}\mathbf{P}\mathbf{Q}^T$.

Proof See [1, 3]. $\qquad\square$

Lemma 3.8 *Suppose that $H_m(v)$ is given in* (10), *we have*

$$\int_0^v H_m(u)\,dB(u) \simeq \frac{1}{m}\mathbf{Q}\mathbf{P}_B\mathbf{Q}^T H_m(v) = \Lambda_B H_m(v),$$

where $\mathbf{Q}$ and $\mathbf{P}_B$ are respectively given in (11) *and Lemma* 3.3 *and $\Lambda_B = \frac{1}{m}\mathbf{Q}\mathbf{P}_B\mathbf{Q}^T$.*

Proof See [1, 3]. $\qquad\square$

4 Numerical method

For convenience, we set $m_1 = m_2 = m$ and nonlinear SIVIE (1) can be solved by HWs. Firstly, a useful result for HWs is proved.

Theorem 4.1 *For the analytic functions $\sigma(v) = \sum a_j v^j$, $\rho(v) = \sum b_j v^j$ and j is a positive integer, then*

$$\sigma\big(x_m(v)\big) = \sigma^T(C_m)H_m(v),$$
$$\rho\big(x_m(v)\big) = \rho^T(C_m)H_m(v),$$

where $H_m(v)$ and C_m are derived in (10),

$$\sigma^T(C_m) = \big(\sigma(c_0), \sigma(c_1), \ldots, \sigma(c_{m-1})\big),$$
$$\rho^T(C_m) = \big(\rho(c_0), \rho(c_1), \ldots, \rho(c_{m-1})\big).$$

Proof According to the disjointness property of HWs, we can deduce

$$
\begin{aligned}
\sigma\left(x_m(v)\right) &= \sum a_j \left(x_m(v)\right)^j \\
&= \sum a_j \left(c_0 h_0(v) + c_1 h_1(v) + \cdots + c_{m-1} h_{m-1}(v)\right)^j \\
&= \sum a_j \left(c_0^j, c_1^j, \ldots, c_{m-1}^j\right) H_m(v) \\
&= \sigma^T(C_m) H_m(v),
\end{aligned}
$$

thus,

$$
\sigma\left(x_m(v)\right) = \sigma^T(C_m) H_m(v) = H_m^T(v) \sigma(C_m). \tag{12}
$$

Similarly,

$$
\rho\left(x_m(v)\right) = \rho^T(C_m) H_m(v) = H_m^T(v) \rho(C_m). \tag{13}
$$

The proof is completed. □

Now, in order to solve (1), we approximate $x(v)$, $x_0(v)$, $k(u,v)$, and $r(u,v)$ in following forms by HWs:

$$
x(v) \simeq x_m(v) = C_m^T H_m(v) = H_m^T(v) C_m, \tag{14}
$$

$$
x_0(v) \simeq x_{0_m}(v) = C_{0_m}^T H_m(v) = H_m^T(v) C_{0m}, \tag{15}
$$

$$
k(u,v) \simeq k_m(u,v) = H_m^T(u) \mathbf{K} H_m(v) = H_m^T(v) \mathbf{K}^T H_m(u), \tag{16}
$$

$$
r(u,v) \simeq r_m(u,v) = H_m^T(u) \mathbf{R} H_m(v) = H_m^T(v) \mathbf{R}^T H_m(u), \tag{17}
$$

where C_m and C_{0m} are HWs coefficient vectors, $\mathbf{K}$ and $\mathbf{R}$ are HWs coefficient matrices. Substituting approximations (12)–(17) into (1), we have

$$
\begin{aligned}
C_m^T H_m(v) = {}& C_{0_m}^T H_m(v) + H_m^T(v) \mathbf{K}^T \int_0^v H_m(u) H^T(u) \sigma(C_m)\, du \\
&+ H_m^T(v) \mathbf{R}^T \int_0^v H_m(u) H_m^T(u) \rho(C_m)\, dB(u).
\end{aligned}
$$

By Lemma 3.3, we get

$$
\begin{aligned}
C_m^T H_m(v) = {}& C_{0_m}^T H_m(v) + H_m^T(v) \mathbf{K}^T \int_0^v \sigma(\tilde{C}_m) H_m(u)\, du \\
&+ H_m^T(v) \mathbf{R}^T \int_0^v \rho(\tilde{C}_m) H_m(u)\, dB(u).
\end{aligned}
$$

Applying Lemmas 3.7 and 3.8, we get

$$
C_m^T H_m(v) = C_{0_m}^T H_m(v) + H_m^T(v) \mathbf{K}^T \sigma(\tilde{C}_m) \boldsymbol{\Lambda} H_m(v) + H_m^T(v) \mathbf{R}^T \rho(\tilde{C}_m) \boldsymbol{\Lambda}_B H_m(v),
$$

then by Lemma 3.4, we derive

$$C_m^T H(v) = C_{0_m}^T H(v) + \hat{\mathbf{A}}_0^T H(v) + \hat{\mathbf{B}}_0^T H(v), \tag{18}$$

where $\mathbf{A}_0 = \mathbf{K}^T \boldsymbol{\sigma}(\tilde{C}_m)\boldsymbol{\Lambda}$ and $\mathbf{B}_0 = \mathbf{R}^T \boldsymbol{\rho}(\tilde{C}_m)\boldsymbol{\Lambda}_B$.

For nonlinear equation (18), a series of methods, such as simple trapezoid method, Simpson method, and Romberg method, are often introduced in the numerical analysis courses. In this paper, the function of fsolve in MATLAB is used to solve equation (18).

5 Error analysis

In contrast to the articles [1, 3], we will give a strict and accurate error analysis in this section. Firstly, we recall two useful lemmas.

Lemma 5.1 *Suppose that function $x(u)$, $u \in [0, 1)$ satisfies the bounded condition and $e(u) = x(u) - x_m(u)$, where $x_m(u)$ is m approximations of HWs of $x(u)$, then*

$$\|e\|_{L^2([0,1))}^2 = \int_0^1 e^2(u)\,du \leq O(h^2). \tag{19}$$

Proof See [1]. □

Lemma 5.2 *Suppose that the function $x(u, v)$ satisfying the bounded condition is defined on $\mathbf{D} = [0, 1) \times [0, 1)$ and $e(u, v) = x(u, v) - x_m(u, v)$, where $x_m(u, v)$ is m approximations of HWs of $x(u, v)$, then*

$$\|e\|_{L^2(\mathbf{D})}^2 = \int_0^1 \int_0^1 e^2(u, v)\,du\,dv \leq O(h^2). \tag{20}$$

Proof See [1]. □

Secondly, let $e(v) = x(v) - x_m(v)$, where $x_m(v)$, $x_{0_m}(v)$, $k_m(u, v)$, and $r_m(u, v)$ are m approximations of Haar wavelets of $x(v)$, $x_0(v)$, $k(u, v)$, and $r(u, v)$, respectively.

$$
\begin{aligned}
e(v) &= x(v) - x_m(v) \\
&= x_0(v) - x_{0_m}(v) \\
&\quad + \int_0^v \left[k(u, v)\sigma\big(x(u)\big) - k_m(u, v)\sigma\big(x_m(u)\big) \right] du \\
&\quad + \int_0^v \left[r(u, v)\rho\big(x(u)\big) - r_m(u, v)\rho\big(x_m(u)\big) \right] dB(u).
\end{aligned} \tag{21}
$$

Lastly, the main convergence theorem is proved.

Theorem 5.1 *Suppose that analytic functions σ and ρ satisfy the following conditions*:
  (i) $|\sigma(x) - \sigma(y)| \leq l_1|x - y|$, $|\rho(x) - \rho(y)| \leq l_3|x - y|$;
  (ii) $|\sigma(x)| \leq l_2$, $|\rho(y)| \leq l_4$;
  (iii) $|k(u, v)| \leq l_5$, $|r(u, v)| \leq l_6$,

where $x, y \in \mathbb{R}$, constant $l_i > 0$, $i = 1, 2, \ldots, 6$. Then

$$\int_0^T \mathbb{E}\big(|e_m(v)|^2\big)\,dv = \int_0^T \mathbb{E}\big(|x(v) - x_m(v)|^2\big)\,dv \le O\big(h^2\big), \quad T \in [0, 1).$$

Proof For (21), we have

$$
\begin{aligned}
\mathbb{E}\big(|e_m(v)|^2\big) \le 3\Bigg[& \mathbb{E}\big(|x_0(v) - x_{0_m}(v)|^2\big) \\
& + \mathbb{E}\left(\left|\int_0^v \big(k(u, v)\sigma\big(x(u)\big) - r_m(u, v)\sigma\big(x_m(u)\big)\big)\,du\right|^2\right) \\
& + \mathbb{E}\left(\left|\int_0^v \big(r(u, v)\rho\big(x(u)\big) - r_m(u, v)\rho\big(x_m(u)\big)\big)\,dB(u)\right|^2\right)\Bigg].
\end{aligned}
$$

On the basis of Lipschitz continuity, Itô isometry, and Cauchy–Schwarz inequality, it yields

$$
\begin{aligned}
\mathbb{E}\big(|e_m(v)|^2\big) \le {} & 3\Bigg[\mathbb{E}\big(|x_0(v) - x_{0_m}(v)|^2\big) \\
& + \mathbb{E}\left(\int_0^v \big|k(u, v)\sigma\big(x(u)\big) - k_m(u, v)\sigma\big(x_m(u)\big)\big|^2\,du\right) \\
& + \mathbb{E}\left(\int_0^v \big|r(u, v)\rho\big(x(u)\big) - r_m(u, v)\rho\big(x_m(u)\big)\big|^2\,du\right)\Bigg] \\
= {} & 3\Bigg[\mathbb{E}\big(|x_0(v) - x_{0_m}(v)|^2\big) \\
& + \int_0^v \mathbb{E}\big(\big|k(u, v)\big(\sigma\big(x(u)\big) - \sigma\big(x_m(u)\big)\big) \\
& \quad + \sigma\big(x_m(u)\big)\big(k(u, v) - k_m(u, v)\big)\big|^2\big)\,du \\
& + \int_0^v \mathbb{E}\big(\big|r(u, v)\big(\rho\big(x(u)\big) - \rho\big(x_m(u)\big)\big) \\
& \quad + \rho\big(x_m(u)\big)\big(r(u, v) - r_m(u, v)\big)\big|^2\big)\,du \Bigg] \\
\le {} & 3\Bigg[\big|x_0(v) - x_{0_m}(v)\big|^2 \\
& + 2{l_1}^2{l_5}^2 \int_0^v \mathbb{E}\big(|e_m(u)|^2\big)\,du + 2{l_2}^2 \int_0^v \big|k(u, v) - k_m(u, v)\big|^2\,du \\
& + 2{l_3}^2{l_6}^2 \int_0^v \mathbb{E}\big(|e_m(u)|^2\big)\,du + 2{l_4}^2 \int_0^v \big|r(u, v) - r_m(u, v)\big|^2\,du \Bigg].
\end{aligned}
$$

Then we can get

$$
\begin{aligned}
\mathbb{E}\big(|e_m(v)|^2\big) \le {} & 3\Bigg[\big|x_0(v) - x_{0_m}(v)\big|^2 + 2{l_2}^2 \int_0^v \big|k(u, v) - k_m(u, v)\big|^2\,du \\
& + 2{l_4}^2 \int_0^v \big|r(u, v) - r_m(u, v)\big|^2\,du \Bigg] \\
& + 6\big({l_1}^2{l_5}^2 + {l_3}^2{l_6}^2\big) \int_0^v \mathbb{E}\big(|e_m(u)|^2\big)\,du,
\end{aligned}
$$

or

$$\mathbb{E}\big(\big|e_m(v)\big|^2\big) \leq \beta(v) + \alpha \int_0^v \mathbb{E}\big(\big|e_m(u)\big|^2\big)\,du,$$

$$\beta(v) = 3\Bigg[\big|x_0(v) - x_{0_m}(v)\big|^2$$

$$+ 2l_2{}^2 \int_0^v \big|k(u,v) - k_m(u,v)\big|^2\,du + 2l_4{}^2 \int_0^v \big|r(u,v) - r_m(u,v)\big|^2\,du\Bigg],$$

$$\alpha = 6\big(l_1{}^2 l_5{}^2 + l_3{}^2 l_6{}^2\big).$$

Let $f(v) = \mathbb{E}(|e_m(v)|^2)$, we get

$$f(v) \leq \beta(v) + \alpha \int_0^v f(\tau)\,d\tau, \quad \tau \in [0, v).$$

By Gronwall's inequality, it follows that

$$f(v) \leq \beta(v) + \alpha \int_0^v e^{\alpha(v-\tau)} \beta(\tau)\,d\tau, \quad v \in [0, 1).$$

Then

$$\int_0^T f(v)\,dv$$

$$= \int_0^T \mathbb{E}\big(\big|e_m(v)\big|^2\big)\,dv$$

$$\leq \int_0^T \bigg(\beta(v) + \alpha \int_0^v e^{\alpha(v-\tau)} \beta(\tau)\,d\tau\bigg)\,dv$$

$$= \int_0^T \beta(v)\,dv + \alpha \int_0^T \int_0^v e^{\alpha(v-\tau)} \beta(\tau)\,d\tau\,dv$$

$$\leq \int_0^T \beta(v)\,dv + \alpha e^{\alpha T} \int_0^T \int_0^v \beta(\tau)\,d\tau\,dv$$

$$= 3\int_0^T \big|x_0(v) - x_{0_m}(v)\big|^2\,dv + 6l_2{}^2 \int_0^T \int_0^v \big|k(u,v) - k_m(u,v)\big|^2\,du\,dv$$

$$+ 6l_4{}^2 \int_0^T \int_0^v \big|r(u,v) - r_m(u,v)\big|^2\,du\,dv$$

$$+ \alpha e^{\alpha T}\Bigg[3 \int_0^T \int_0^v \big|x_0(\tau) - x_{0_m}(\tau)\big|^2\,d\tau\,dv$$

$$+ 6l_2{}^2 \int_0^T \int_0^t \int_0^\tau \big|k(s,\tau) - k_m(s,\tau)\big|^2\,ds\,d\tau\,dt$$

$$+ 6l_4{}^2 \int_0^T \int_0^v \int_0^\tau \big|r(u,\tau) - r_m(u,\tau)\big|^2\,du\,d\tau\,dv\Bigg]$$

$$= 3I_1 + 6l_2^2 I_2 + 6l_4^2 I_3 + \alpha e^{\alpha T}\big[3I_4 + 6l_2^2 I_5 + 6l_4^2 I_6\big].$$

By using (19) and (20), we have

$$I_i \leq w_i h^2, \quad i = 1, 2, \ldots, 6.$$

So we can get

$$\int_0^T \mathbb{E}\big|e_m(v)\big|^2 \, dv \leq \big[\big(3w_1 + 6l_2{}^2 w_2 + 6l_4{}^2 w_3\big) + \alpha e^{\alpha T}\big(3w_4 + 6l_2{}^2 w_5 + 6l_4{}^2 w_6\big)\big]h^2$$

$$\leq O\big(h^2\big),$$

where constant $w_i > 0$, $i = 1, 2, \ldots, 6$.

The proof is completed. □

6 Numerical examples

In this section, some examples are given to verify the validity and rationality of the above method.

Table 1 When $m = 2^4$, error means E_m, error standard deviations E_s, and confidence intervals are given in this table

v	E_m	E_s	95% confidence interval for error mean	
			Lower	Upper
$\frac{1}{16}$	2.1422688×10^{-5}	1.0711344×10^{-6}	8.4307964×10^{-8}	4.2416924×10^{-6}
$\frac{2}{16}$	6.9693462×10^{-5}	3.4846731×10^{-6}	1.7016633×10^{-7}	1.3799305×10^{-5}
$\frac{3}{16}$	6.0556726×10^{-5}	3.0278363×10^{-6}	1.4766843×10^{-7}	1.1990231×10^{-5}
$\frac{4}{16}$	5.9652419×10^{-5}	2.9826209×10^{-7}	2.1384868×10^{-7}	1.1811179×10^{-5}
$\frac{5}{16}$	2.9736896×10^{-5}	1.4868448×10^{-6}	$6.69011884 \times 10^{-8}$	5.8879054×10^{-6}

Table 2 When $m = 2^5$, error means E_m, error standard deviations E_s, and confidence intervals are given in this table

| v	E_m	E_s	95% confidence interval for error mean	
			Lower	Upper
$\frac{1}{32}$	2.2590513×10^{-6}	1.1295256×10^{-6}	4.5181026×10^{-8}	4.4729216×10^{-6}
$\frac{2}{32}$	8.7823046×10^{-6}	4.3911523×10^{-6}	1.7564609×10^{-7}	1.7388963×10^{-5}
$\frac{3}{32}$	1.1192231×10^{-5}	5.5961158×10^{-6}	2.2384463×10^{-7}	2.2160618×10^{-5}
$\frac{4}{32}$	1.1983301×10^{-5}	5.9916507×10^{-6}	2.3966603×10^{-7}	2.3726937×10^{-5}
$\frac{5}{32}$	3.9319526×10^{-5}	1.9659763×10^{-5}	7.8639053×10^{-7}	7.7852663×10^{-6}

**Figure 1** $m = 2^4$, simulation result of the approximate solution and exact solution for Example 6.1
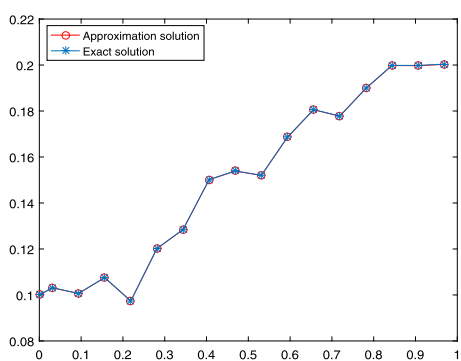
Figure 2 $m = 2^5$, simulation result of the approximate solution and exact solution for Example 6.1
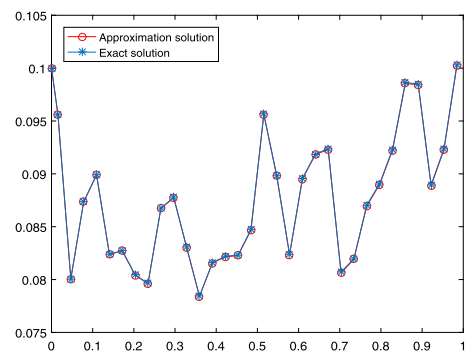
Figure 3 $m = 2^4$, simulation result of the approximate solution and mean solution for Example 6.2
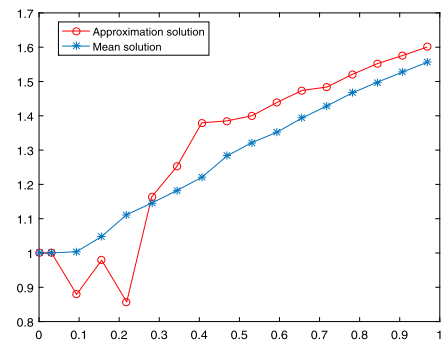
Figure 4 $m = 2^5$, simulation result of the approximate solution and mean solution for Example 6.2
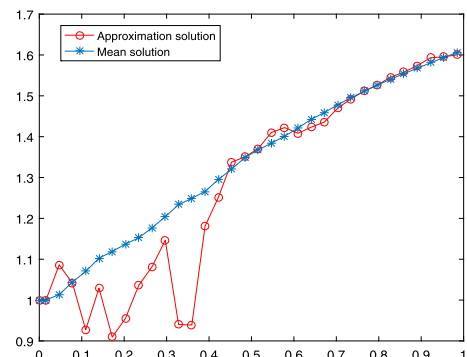
Example 6.1 Consider the nonlinear SIVIE [6, 8]

$$x(v) = x_0(v) - a^2 \int_0^v x(u)\bigl(1 - x^2(u)\bigr)\, du + a \int_0^v \bigl(1 - x^2(u)\bigr)\, dB(u), \quad v \in [0,1),$$

where

$$x(v) = \tanh\bigl(aB(v) + \operatorname{arctanh}(x_0)\bigr).$$

In this example, $a = \frac{1}{30}$ and $x_0(v) = \frac{1}{10}$. The error means E_m, error standard deviations E_s, and confidence intervals of Example 6.1 for $m = 2^4$ and $m = 2^5$ are shown in Table 1 and Table 2, respectively. The error means E_m and error standard deviations E_s are obtained by 10^4 trajectories. Compared with Table 2 in [8], E_m is smaller and the confidence

interval is smaller under the same confidence level. Moreover, the comparison of exact and approximate solutions of Example 6.1 for $m = 2^4$ and $m = 2^5$ is displayed in Fig. 1 and Fig. 2, respectively.

Example 6.2 Consider the nonlinear SIVIE [17, 18]

$$x(v) = 1 + \int_0^v e^{-(v-u)} \sin\big(x(u)\big)\, du + \int_0^v e^{-(v-u)} \cos\big(x(u)\big)\, dB(u), \quad v \in [0,1).$$

The mean and approximate solutions of Example 6.2 for $m = 2^4$ and $m = 2^5$ are respectively given in Fig. 3 and Fig. 4, where the mean solution is obtained by 10^4 trajectories.

Publisher's Note
Springer Nature remains neutral with regard to jurisdictional claims in published maps and institutional affiliations.

References
1. Mohammadi, F.: Numerical solution of stochastic Itô–Voltterra integral equations using Haar wavelets. Numer. Math., Theory Methods Appl. **9**, 416–431 (2016)
2. Reihani, M.H., Abadi, Z.: Rationalized Haar functions method for solving Fredholm and Volterra integral equations. J. Comput. Appl. Math. **200**, 12–20 (2007)
3. Maleknejad, K., Khodabin, M., Rostami, M.: Numerical solution of stochastic Volterra integral equation by a stochastic operational matrix based on block pulse function. Math. Comput. Model. **55**, 791–800 (2012)
4. Maleknejad, K., Basirat, B., Hashemizadeh, E.: Hybrid Legendre polynomials and block-pulse functions approach for nonlinear Volterra–Fredholm integro-differential equations. Comput. Math. Appl. **61**, 2821–2828 (2011)
5. Maleknejad, K., Khodabin, M., Rostami, M.: A numerical method for solving m-dimensional stochastic Itô–Volterra integral equations by stochastic operational matrix. Comput. Math. Appl. **63**, 133–143 (2012)
6. Ezzati, R., Khodabin, M., Sadati, Z.: Numerical implementation of stochastic operational matrix driven by a fractional Brownian motion for solving a stochastic differential equation. Abstr. Appl. Anal. **2014**, Article ID 523163 (2014)
7. Jiang, G., Sang, X.Y., Wu, J.H., Li, B.W.: Numerical solution of two-dimensional nonlinear stochastic Itô–Volterra integral equations by applying block pulse function. Adv. Pure Math. **9**, 53–66 (2019)
8. Hashemi, B., Khodabin, M., Maleknejad, K.: Numerical solution based on hat functions for solving nonlinear stochastic Itô–Volterra integral equations driven by fractional Brownian motion. Mediterr. J. Math. **14**, 1–15 (2017)
9. Heydari, M.H., Hooshmandasl, M.R., Ghaini, F.M.M., Cattani, C.: A computational method for solving stochastic Itô–Volterra integral equations based on stochastic operational matrix for generalized hat basis functions. Mediterr. J. Math. **270**, 402–415 (2014)
10. Mirzaee, F., Hadadiyan, E.: Numerical solution of Volterra–Fredholm integral equations via modification of hat functions. Appl. Math. Comput. **280**, 110–123 (2016)
11. Balakumar, V., Murugesan, K.: Single-term Walsh series method for systems of linear Volterra integral equations of the second kind. Appl. Math. Comput. **228**, 371–376 (2014)
12. Blyth, W.F., May, R.L., Widyaningsih, P.: Volterra integral equations solved in Fredholm form using Walsh functions. ANZIAM J. **45**, 269–282 (2003)
13. Mohamed, D.S., Taher, R.A.: Comparison of Chebyshev and Legendre polynomials methods for solving two dimensional Volterra–Fredholm integral equations. J. Egypt. Math. Soc. **25**, 302–307 (2017)
14. Maleknejad, K., Sohrabi, S., Rostami, Y.: Numerical solution of nonlinear Volterra integral equations of the second kind by using Chebyshev polynomials. Appl. Math. Comput. **188**, 123–128 (2007)
15. Ezzati, R., Najafalizadeh, S.: Application of Chebyshev polynomials for solving nonlinear Volterra–Fredholm integral equations system and convergence analysis. Indian J. Sci. Technol. **5**, 2060–2064 (2012)
16. Asgari, M., Hashemizadeh, E., Khodabin, M., Maleknejad, K.: Numerical solution of nonlinear stochastic integral equation by stochastic operational matrix based on Bernstein polynomials. Bull. Math. Soc. Sci. Math. Roum. **57105**, 3–12 (2014)

17. Zhang, X.C.: Euler schemes and large deviations for stochastic Volterra equations with singular kernels. J. Differ. Equ. **244**, 2226–2250 (2008)
18. Zhang, X.C.: Stochastic Volterra equations in Banach spaces and stochastic partial differential equation. J. Funct. Anal. **258**, 1361–1425 (2010)